

Systematic differences in simple stellar population model results: Application to the M31 globular-like cluster system

Z. Fan^{1*} and R. de Grijs^{2,3†}

¹Key Laboratory of Optical Astronomy, National Astronomical Observatories, Chinese Academy of Sciences, A20 Datun Road, Chaoyang District, Beijing 100012, China

²Kavli Institute for Astronomy and Astrophysics, Peking University, Yi He Yuan Lu 5, Hai Dian District, Beijing 100871, China

³Department of Astronomy and Space Science, Kyung Hee University, Yongin-shi, Kyungki-do 449-701, Republic of Korea

Received; Accepted

ABSTRACT

Simple stellar population (SSP) synthesis models are useful tools for studying the nature of unresolved star clusters in external galaxies. However, the plethora of currently available SSP models gives rise to significant and poorly documented systematic differences. Here we consider the outputs of the commonly used Bruzual & Charlot and GALEV models, as well as a recently updated SSP model suite which attempts to include the contributions of binary merger products in the form of blue straggler stars (BS-SSP). We rederive the ages, metallicities, extinction values and masses of 445 previously observed globular-like clusters in M31 based on χ^2 minimisation of their spectral energy distributions with respect to these three different SSP models and adopting a Chabrier-like stellar initial mass function. A comparison between our new results and previous estimates of the same parameters shows that the Bruzual & Charlot models yield the youngest ages and lowest masses, while adoption of the BS-SSP models results in the oldest ages and highest mass estimates. Similarly, the GALEV SSP models produce the lowest metallicities, with the highest values resulting from the BS-SSP model suite. These trends are caused by intrinsic differences associated with the models, and are not significantly affected by the well-known age–metallicity degeneracy. Finally, we note that the mass function of the massive M31 star clusters is similar to that of the Milky Way’s globular clusters, which implies that the two star cluster systems likely formed under similar environmental conditions.

Key words: galaxies: individual (M31) – galaxies: star clusters – globular clusters: general – methods: data analysis

1 INTRODUCTION

Star clusters represent an important stellar population component of galaxies. Their age distributions trace the main evolutionary events associated with the formation and evolution of their host galaxies. However, most clusters in external galaxies cannot be resolved into individual stars, even with the superb resolution of the *Hubble Space Telescope* (*HST*). Consequently, stellar population synthesis has become an important and powerful tool to interpret the nature of extragalactic star clusters, including their ages, metallicities, reddening values and masses. In the past few decades, many different simple stellar population (SSP) synthesis models have been constructed and applied to study extragalactic star clusters based on photometry in multiple passbands, including Bruzual & Charlot (1993); Worthey (1994); Leitherer & Heckman (1995); Fioc & Rocca-Volmerange

(1997); Maraston (1998); Vazdekis (1999); Bruzual & Charlot (2003); Yi et al. (2003); Maraston (2005); Conroy et al. (2009); Xin et al. (2011), as well as the GALEV models (see, e.g., Schulz et al. 2002, 2003; Anders & Fritze-v. Alvensleben 2003; Fritze-v. Alvensleben & Bicker 2006; Kotulla et al. 2009). The recently updated BS-SSP models (Xin et al. 2011) considered the effects of blue straggler stars (BSs), which are likely the products of binary mergers and which seem a common occurrence in star clusters (see, e.g., Ahumada & Lapasset 1995; Piotto et al. 2002; Xin et al. 2011). Since BSs are often luminous and can render the integrated luminosities and colours of their host clusters significantly brighter and bluer, we set out to explore the differences between results derived from application of the BS-SSP models and those derived from other models. Here we choose two commonly used models – Bruzual & Charlot (2003, henceforth BC03) and GALEV – for our comparisons.

Star clusters were long thought of as members of two distinct types, i.e., open clusters (OCs) and globular clusters (GCs). OCs are generally young, not very massive, faint, diffuse, and usually

* E-mail: zfan@bao.ac.cn
† E-mail: grijs@pku.edu.cn

located in galactic discs, quite contrary to the nature of GCs, which are mostly old, massive, luminous, centrally concentrated, and usually located in the haloes of their host galaxies. However, this simplistic picture has been changing since the discovery of young massive star clusters (YMCs) in many galaxies, including in the Milky Way (e.g., Ascenso et al. 2007a,b), M31 (e.g., Barmby et al. 2009; Caldwell et al. 2009; Ma et al. 2009; Perina et al. 2009, 2010; Hodge et al. 2010), M82 (e.g., O’Connell & Mangan 1978; de Grijs et al. 2003a; Smith et al. 2007; McCrady 2009), the Antennae galaxies (e.g., Whitmore et al. 2005) and NGC 1140 (e.g., Hunter et al. 1994; de Grijs et al. 2004; Moll et al. 2008) as well as NGC 3603 and R136 (Maíz Apellániz 2009). YMC properties span those of both OCs and GCs, with typical masses ($> 10^4 M_{\odot}$) greater than those of (most) OCs and young ages (< 1 Gyr), i.e., quite different from present-day GCs, so that they are often considered candidate proto-GCs. The new category of YMCs renders cluster classification blurred and difficult. In this paper, we use the term ‘globular-like’ cluster to distinguish massive (YMCs and GCs) from lower-mass clusters (OCs). Since OCs are usually faint and located in galactic discs, this makes them difficult to study, which is why we focus on globular-like clusters here.

Located at a distance of ~ 780 kpc (Stanek & Garnavich 1998; Macri 2001; McConnachie et al. 2005), M31 is the nearest large spiral galaxy in our Local Group of galaxies. Therefore, it represents an ideal laboratory for studies of statistically significant numbers of globular-like clusters in external galaxies. In addition, since the Hubble type and mass of M31 are similar to those of our Galaxy, studying M31’s massive cluster system is also important for our understanding of the Galactic GC system. Based on *HST* Wide Field and Planetary Camera-2 (WFPC2) images, Krienke & Hodge (2007) suggested that there may be $\sim 80,000$ star clusters in the M31 disc. Most of these disc clusters are faint OCs. The number of GCs in M31 is much smaller. Barmby & Huchra (2001) estimated their total number at 460 ± 70 , while Perina et al. (2010) arrived at ~ 530 , with an additional ~ 100 YMCs. To limit the scope of this paper, we only focus on the globular-like clusters, including GCs and YMCs, because they are luminous and relatively easy to observe at the distance of M31. Studies aimed at identification, classification and analysis of the population of M31 globular-like clusters have been undertaken since the pioneering work of Hubble (1932) (see, e.g., Vetešnik 1962; Sargent et al. 1977; Battistini et al. 1980, 1987, 1993; Crampton et al. 1985; Barmby et al. 2000).

Application of the χ^2 -minimisation technique to spectral-energy-distribution (SED) fitting is a commonly used method for estimating ages, metallicities, reddening values and masses of extragalactic star clusters (see, e.g., Jiang et al. 2003; de Grijs et al. 2003a,b, 2005; de Grijs & Anders 2006; Fan et al. 2006; Ma et al. 2007, 2009; Wang et al. 2010). The M31 massive star cluster system has also been studied extensively in this manner. For instance, Jiang et al. (2003) studied 172 GCs from the Battistini et al. (1987) sample which were located in the central $\sim 1 \text{ deg}^2$ region of the image and observed by the Beijing–Arizona–Taipei–Connecticut (BATC; see Fan et al. 1996) survey. The observations of all of these clusters had relatively high signal-to-noise ratios (S/N) – and thus good photometry – in the 13 BATC intermediate-band filters covering the range from $\sim 4,000$ to $\sim 10,000 \text{ \AA}$. By comparison of their SEDs with the SSP models of Bruzual & Charlot (1996; unpublished, updated version of Bruzual & Charlot 1993), Jiang et al. (2003) concluded that nearly all their sample GCs were older than 1 Gyr. (Note that their sample GCs were mainly selected from the M31 bulge and inner disc, while they only used three differ-

ent metallicities for their comparisons.) Fan et al. (2006) estimated the ages of 91 GCs in M31 from the Jiang et al. (2003) sample by matching BATC intermediate-band and Two-Micron All-Sky Survey (2MASS) *JHK* SEDs with BC03 SSP models. They identified a young, ~ 3 Gyr-old population and an intermediate-age population of ~ 8 Gyr, in addition to the well-known old (> 10 Gyr) GC population.

It has been unequivocally established that near-infrared (NIR) photometry can partially break the age–metallicity degeneracy and, hence, improve age estimates (e.g., Anders et al. 2004b). Ma et al. (2007) determined the age of an old M31 globular-like cluster (S312) based on *GALEX* near-ultraviolet, optical broad-band, BATC and 2MASS *JHK* photometry. They concluded that this cluster has a mass of $(9.8 \pm 1.85) \times 10^5 M_{\odot}$ and an age of 9.5 Gyr. Subsequently, Ma et al. (2009) used the *GALEX* SSP models applied to BATC, 2MASS *JHK* and *GALEX* data to derive the ages of 35 GCs in the central M31 field that were not included in Jiang et al. (2003). These clusters were also selected from Battistini et al. (1987) and located in the galaxy’s central $\sim 1 \text{ deg}^2$, but most of their observations were characterised by relatively poor S/Ns. (Note that the *GALEX* SSP models provide spectral templates for ages up to 16 Gyr and metallicities $Z > 0.0004$, while the BC03 models include ages up to 20 Gyr, so that minor differences may result for the oldest and lowest-metallicity ($Z < 0.0004$) clusters, depending on the SSP model suite adopted.) Ma et al. (2009) found that most of their sample GCs covered the age range from 1 to 6 Gyr, with a peak at ~ 3 Gyr. Recently, Wang et al. (2010) performed photometry of another 104 M31 globular-like clusters using BATC multicolour observations of the central $\sim 6 \text{ deg}^2$ M31 field, which covers a large part of the galactic disc, where many young star clusters can be found. They estimated the clusters’ ages by fitting their SEDs with *GALEX* SSP models, revealing the presence of young, intermediate-age and old cluster populations in M31. All of these studies were based on SED fitting of multicolour photometry and comparison with SSP models.

Despite a significant historical body of work and the large number and diversity of currently available SSP models, systematic differences among model outputs persist. For instance, Peacock et al. (2011) recently compared several SSP models with photometry obtained through the Sloan Digital Sky Survey filters of M31 globular-like clusters. They identified a significant offset between the models and the observed ($g - r$) colours. Conroy et al. (2009) investigated the propagation of uncertainties in stellar population synthesis modelling, and specifically their impact on our understanding of the observational manifestations of stellar evolution, the stellar initial mass function (IMF) and the luminosity evolution of stars and stellar populations. They found that stellar masses could be affected by errors of ~ 0.3 dex in nearby galaxies, while for more distant bright red galaxies, the uncertainties in mass are at the ~ 0.6 dex level. Conroy & Gunn (2010) compared and assessed the differences in the luminosities and colours of their stellar population synthesis models (FSPS) with respect to those associated with both the BC03 and Maraston (2005) (M05) model suites. They found that the FSPS and BC03 models perform well for star clusters in the Magellanic Clouds, while the M05 models seem to be too red and result in incorrect age dependences. However, all three models provide poor fits to the NIR colours of star clusters in both the Galaxy and M31. They also found that the FSPS models can fit ultraviolet photometry successfully, while the BC03 and M05 models fail in doing so. Recently, Maraston & Stromback (2011) compared the colour indices and spectral profiles of their models based on application of different empirical stellar spectral libraries,

including the observational Pickles, ELODIE, STELIB and MILES libraries, the theoretical MARCS stellar library, and the models of Vazdekis et al. (2010) and Conroy & Gunn (2010). They noted that SSP models based on empirical libraries have lower fluxes in the V band than theoretically predicted by the BaSeL spectral library (Lejeune, Cuisinier & Buser 1997, 1998), which in turn is based on the Kurucz (1992) library. This could lead to bluer ($B - V$) colours (by up to 0.05 mag) in their models. In this paper, we aim at exploring the causes and extents of systematic effects resulting from application of specific sets of SSP models to broad-band photometric observations. This paper builds on our previous work in characterising uncertainties owing to application of SSP models to broad-band SEDs, in particular Anders et al. (2004b), de Grijs et al. (2005) and de Grijs & Anders (2006). Although a small fraction ($\lesssim 5\%$) of our sample clusters have masses \lesssim a few $\times 10^4 M_{\odot}$, we specifically do not consider the effects of stochastic sampling of the stellar IMF. Stochasticity will increase the uncertainties associated with the resulting model parameters, particularly so for the lower-mass clusters, i.e., \lesssim a few $\times 10^4 M_{\odot}$ (e.g., Cerviño, Luridiana & Castander 2000; Cerviño et al. 2002; Cerviño & Luridiana 2004, 2006; Maíz Apellániz 2009; Popescu & Hanson 2010; Fouesneau & Lançon 2010; Fouesneau et al. 2012; Popescu, Hanson & Elmegreen 2012), but a detailed study of these effects in the context of our current work is beyond the scope of this paper.

Here we derive the ages, metallicities, reddening values and masses of the 445 confirmed globular-like clusters and cluster candidates by comparing the observed SEDs with GALEV models as well as the latest BS-corrected models (Xin et al. 2011) since recent studies show that nearly all star clusters contain so-called blue straggler stars (e.g., Ahumada & Lapasset 1995; Piotto et al. 2002; Xin et al. 2011), which could artificially render the integrated star cluster colours much bluer than their real, intrinsic colours. It is interesting to compare the results from different models, which helps us to better understand the practical impact of the differences between the models. In addition, we compare our BS-SSP and GALEV-based results with those derived using the BC03 model suite. This paper is organized as follows. Sect. 2 describes our sample selection and $UBVRIJHK$ photometry. In Sect. 3, we describe how we fit the SEDs using the different SSP models. Sect. 4 presents the resulting ages, metallicities, masses and their distributions as well as comparisons of the estimates derived based on adoption of different SSP models. Finally, we summarise and conclude the paper in Sect. 5.

2 SAMPLE

Fan et al. (2010) provided the basic globular-like cluster sample and photometry for our work. They performed $UBVRI$ photometry based on archival images of the Local Group Galaxy Survey, which covers a region of 2.2 deg^2 along M31's major axis. The fields were observed from August 2000 to September 2002 with the KPNO Mayall 4 m telescope (for observational details see Massey et al. 2006). The coordinates specified by Caldwell et al. (2009) were used for cluster identification and aperture photometry based on a set of variable aperture radii ranging from 1.03 to 9.06 arcsec. A comparison of this new photometry with that published in the Revised Bologna Catalogue (RBC) v.4 (Galleti et al. 2004, 2006, 2007, 2009), as well as with other data sets (Barmby et al. 2000; Peacock et al. 2010), showed minor to negligible systematic differences, with maximum offsets of 0.1 to 0.2σ , where σ refers to the r.m.s. scatter in the photometric differences. To enlarge

their sample, Fan et al. (2010) also included a small fraction of the $UBVRI$ photometry from the RBC v.4. Thus, the $UBVRI$ cluster photometry adopted in this paper is homogeneous. Fan et al. (2010) also adopted the JHK photometry of Galleti et al. (2009), because NIR photometry is important to (partially) break degeneracies in SED fits (e.g., Anders et al. 2004b). Finally, the authors obtained a sample of 445 confirmed globular-like clusters and cluster candidates with photometry in at least six of the $UBVRIJHK$ bands. They derived the ages, metallicities, masses and reddening values based on the BC03 model suite, using Padova isochrones and a Chabrier IMF. Therefore, we use the sample of Fan et al. (2010) as the basis for our tests and comparisons.

3 METHOD

In this section, we describe the methods and processes used for our redeterminations of the cluster ages, metallicities, extinction values and masses based on SED fitting. The general fitting method used here is the same as that in Fan et al. (2010), although we use different, updated SSP models.

3.1 SSP models used

Since we have access to photometry in optical and NIR broad-band filters from Fan et al. (2010), we can obtain the clusters' fundamental integrated physical parameters, such as their ages, metallicities and masses, by means of SED fitting. However, a large body of evidence suggests that a strong age–metallicity degeneracy dominates if only optical photometry is used (Worthey 1994; Arimoto 1996; Kaviraj et al. 2007). Anders et al. (2004b) concluded that the degeneracy can be partially broken by adding NIR photometry to the optical colours, with the efficacy of this process depending on the age of the stellar population. de Grijs et al. (2005) and Wu et al. (2005) also showed that use of NIR colours can greatly contribute to break the age–metallicity and age–extinction degeneracies. It has also been shown that U -band data is important to obtain accurate age, metallicity and extinction estimates based on SED fits (see, e.g., Anders et al. 2003a, 2004a,b; de Grijs et al. 2005; Gieles et al. 2005; Bastian et al. 2005a,b; Kotulla et al. 2009). Thus, in our fits, we used the full $UBVRI$ photometric data set of Fan et al. (2010), complemented with JHK photometry from the RBC v.4, to disentangle the degeneracies and obtain more reliable results.

We used a χ^2 -minimisation technique for our age, metallicity, mass and extinction estimates, comparing the observed, integrated SEDs with theoretical SSP models (see, e.g., Fan et al. 2006, 2010; Ma et al. 2007, 2009; Wang et al. 2010). In this paper, we take advantage of the availability of a new set of SSP models that attempt to correct for the contributions of BSs (Xin et al. 2011). The BS-SSP model suite is based on the Padova 1994 isochrones and the BaSeL–Kurucz stellar spectral library. We decided to use these BS-SSP models because the (central) cluster colours are often affected by the presence of BSs, thus causing deviations in (predominantly) the U and B bands with respect to SSP models based solely on single-star evolution (Xin & Deng 2005; Xin et al. 2007; Cenarro et al. 2008). Following Xin et al. (2011), we adopt a two-part power-law IMF, similar to both the Chabrier (2003) and Kroupa (2001) formalisms. The BS-SSP synthesis models include five initial metallicities ($Z = 0.0004, 0.004, 0.008, 0.02 = Z_{\odot}$, and 0.05, (corresponding to $[\text{Fe}/\text{H}] = -1.7, -0.7, -1.4, 0$ and $+0.4$ dex), and 24 equally logarithmically-spaced time steps from 100 Myr to 20 Gyr with a wavelength coverage from 91 Å

to 160 μm . To avoid discontinuities, following Fan et al. (2006), Ma et al. (2007), Ma et al. (2009), Wang et al. (2010) and Fan et al. (2010), we linearly interpolated the input metallicities to create a higher-resolution spectral grid containing 100 metallicities (from $[\text{Fe}/\text{H}] = -1.7$ to $+0.4$) and 231 ages from 0.1 Gyr to 20 Gyr, with equally logarithmically-spaced intervals between the newly created templates. Although Frayn & Gilmore (2002) discussed the merits and problems associated with linear interpolation between two points in logarithmic space, which may especially be an issue for sharp ‘hooks’ in our isochrones, Charlot & Bruzual (1991) and Bruzual & Charlot (1993, 2003) suggested that interpolation of the model ages and metallicities is feasible and can be done reasonably well.

The GALAXEV models (BC03) follow the spectral and photometric evolution of SSPs for a wide range of stellar metallicities. The model suite includes 26 SSP models at both high and low resolution, 13 of which were computed using the Chabrier (2003) IMF assuming lower and upper stellar mass cutoffs of $m_L = 0.1$ and $m_U = 100 M_\odot$, respectively. The other 13 models were computed using the Salpeter (1955) IMF with the same mass cutoffs. This model suite provides SSP models based on both the Padova 1994 and 2000 evolutionary tracks. However, the authors point out that the Padova 2000 models tend to produce worse agreement with observed galaxy colours. These SSP models contain 221 ages, in unequally-spaced time steps from 1×10^5 yr to 20 Gyr. The evolving spectra include the contribution of the stellar component at wavelengths from 91 \AA to 160 μm . In this paper, we adopt the high-resolution SSP models computed using the Padova 1994 evolutionary tracks and a Chabrier (2003) IMF. The spectral libraries used include the theoretical BaSeL and observational STELIB and Pickles collections. Fan et al. (2010) linearly interpolated the metallicities provided by the Padova 1994 model grid ($[\text{Fe}/\text{H}] = -2.2490, -1.6464, -0.6392, -0.3300, +0.0932$ and $+0.5595$ dex) using 100 equal steps and fitted the SEDs of the globular-like clusters based on the high-resolution BC03 models. In this paper, we do not redo the fits based on the BC03 models, but we simply adopt the results of Fan et al. (2010).

For the GALEV models, we used the Padova 1994 theoretical isochrones with a Kroupa IMF and the BaSeL library of stellar spectra. Indeed, BC03 showed that the spectral properties based on a Kroupa IMF are very similar to those using the Chabrier IMF. The models include five initial metallicities, $Z = 0.0004, 0.004, 0.008, 0.02$ and 0.05 , corresponding to $[\text{Fe}/\text{H}] = -1.7, -0.7, -0.4, 0$ and $+0.4$ (Anders et al. 2003b) with 4000 equally-spaced time steps from 4 Myr to 16 Gyr (in steps of 4 Myr). In fact, to approximate a comparable resolution in age, we reduced the number of time steps to 200: we kept the model’s original time steps for ages < 1 Gyr and enlarged the time interval to 0.1 Gyr for older ages. The wavelength coverage also spans the range from 91 \AA to 160 μm . Similarly, to achieve higher metallicity resolution and avoid discontinuities, we enlarged the spectral grid – which contained 105 metallicities (from $[\text{Fe}/\text{H}] = -1.7$ to 0.4) – by interpolating in logarithmic space, using equally logarithmically-spaced intervals between the newly created templates, as recommended by Kotulla et al. (2009).

Using Fig. 1, we investigate the *UBVRIJHK* colour behaviour as a function of age as predicted by the different models, i.e., the BS-SSP, BC03 and GALEV models. We adopted solar metallicity and all colours are in the Vega photometric system. The BS-corrected models yield offsets to the blue for all colours: for ages > 2 Gyr, we find colour offsets $(U - B) \sim 0.2$, $(B - V) \sim 0.1$, $(V - R) \sim 0.1$ and $(V - I) \sim 0.1$ mag with respect

to the other models, while for ages < 2 Gyr, the offsets for these same colours are smaller or even negligible. However, the GALEV models exhibit much redder colours in $(V - K)$ and $(J - H)$ for ages < 2 Gyr, which may affect our age estimates of young stellar populations. The GALEV and BC03 models predict similar colours in $(U - B)$, $(B - V)$, $(V - R)$ and $(V - I)$ while the two model sets show significant offsets in $(V - K)$ and $(J - H)$ colours, particularly for young ages.

Figure 2 is similar to Fig. 1 but shows the colours as a function of metallicity for an age of 12 Gyr, where any differences are most prominent. In all panels, we find that the BS-SSP models predict the bluest colours, while the GALEV models predict the reddest colours. Note also that for $(V - R)$, $(V - I)$ and $(J - H)$, the GALEV and BC03 models predict similar colours (within reasonable observational uncertainties) as a function of metallicity.

In Fig. 3 we show the mass-to-light ratios (M/L s) in the *V* band as a function of age for solar metallicity for the three models. The GALEV models predict the highest M/L s, while the BS-SSP models predict the lowest for all ages. In addition, the differences becomes larger for older ages.

These intrinsic colour and M/L differences will lead to differences in the results predicted by the different models. In particular, the BS-SSP models are expected to predict intrinsically older ages, higher metallicities and lower masses for the same age, regardless of the reddening affecting the cluster photometry. Fig. 3 shows that one should be aware that if the ages predicted by BS-SSP models are not sufficiently old, the M/L_V values derived from the BS-SSP models could be lower than those predicted by other models.

3.2 Fitting procedure

The BS-SSP and GALEV spectra can easily be convolved to magnitudes in the AB system using the filter-response functions in the *UBVRIJHK* bands. The apparent magnitudes of the BS-SSP/GALEV synthesis models in the AB system are given by

$$m_{\text{AB}}(t) = -2.5 \log \frac{\int_{\lambda_1}^{\lambda_2} d\lambda \lambda F_\lambda(\lambda, t) R(\lambda)}{\int_{\lambda_1}^{\lambda_2} d\lambda \lambda R(\lambda)} - 48.60, \quad (1)$$

where $R(\lambda)$ is filter-response function and $F_\lambda(\lambda, t)$ the flux, which is a function of wavelength (λ) and evolutionary time (t). λ_1 and λ_2 are the lower and upper wavelength cutoffs of the respective filter (see BC03). We converted all observed integrated magnitudes (*UBVRIJHK*) to the AB system using the Kurucz (1992) SEDs.

Since a comparison of the extinction values of the M31 globular-like clusters from Fan et al. (2008) and Barmby et al. (2000) shows that the offset is -0.01 ± 0.10 , we continued on the assumption that there is no systematic offset between the two data sets. Therefore, for those (310 of 445) clusters in our sample that have reddening values from Fan et al. (2008) or Barmby et al. (2000), the magnitudes were corrected for reddening assuming a Cardelli et al. (1989) Galactic extinction law, so that their ages and metallicities can be determined by comparison of the interpolated high-resolution BC03 SSP synthesis models with the SEDs from our photometry and leaving the metallicity $[\text{Fe}/\text{H}]$ as a free parameter, i.e.,

$$\chi_{\text{min}}^2(t, [\text{Fe}/\text{H}]) = \min \left[\sum_{i=1}^8 \left(\frac{m_{\lambda_i}^{\text{obs}} - m_{\lambda_i}^{\text{mod}}}{\sigma_i} \right)^2 \right], \quad (2)$$

where $m_{\lambda_i}^{\text{mod}}(t, [\text{Fe}/\text{H}])$ is the integrated magnitude in the i^{th} filter of a theoretical SSP at age t and for metallicity $[\text{Fe}/\text{H}]$, $m_{\lambda_i}^{\text{obs}}$

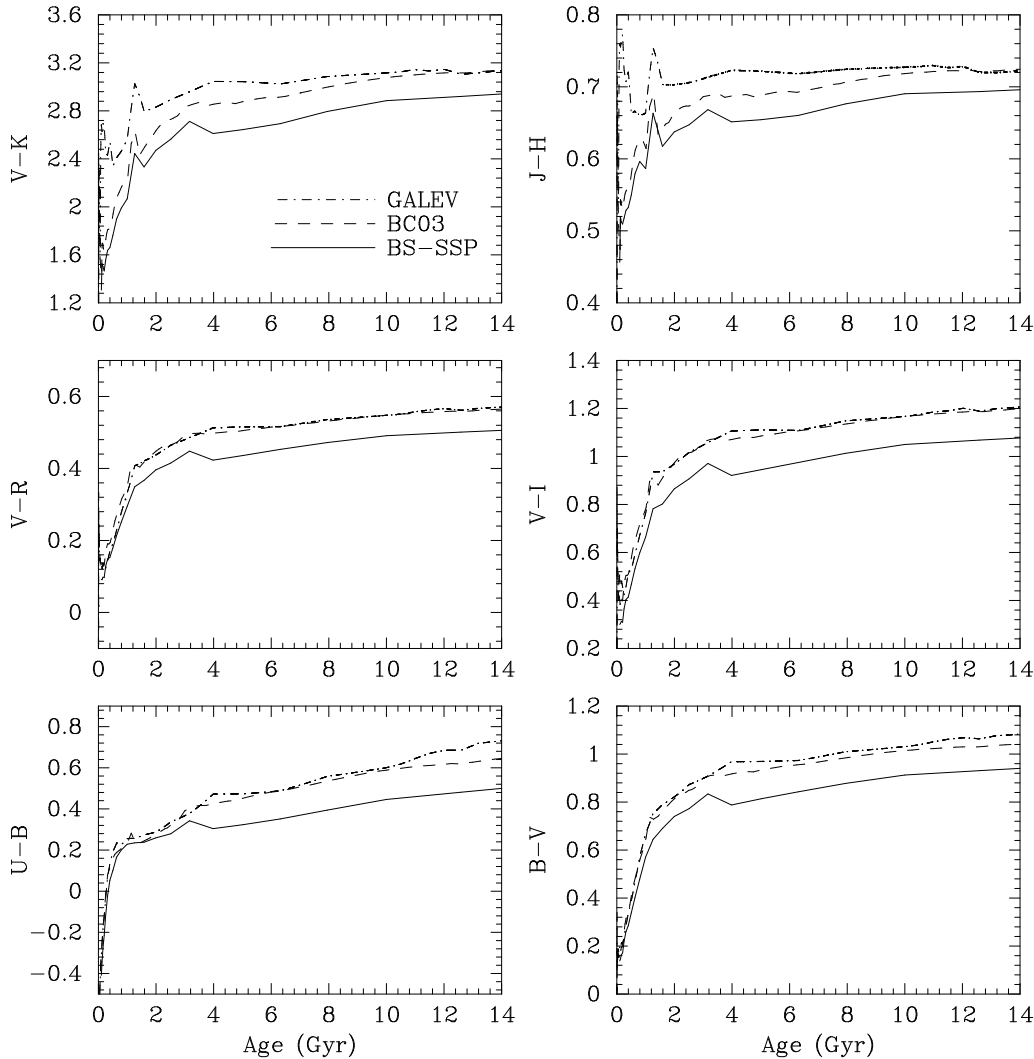


Figure 1. Predicted colours (in the Vega photometric system) as a function of age for solar-metallicity SSPs (solid lines: BS-SSP; dashed lines: BC03; dot-dashed lines: GALEV).

represents the observed, integrated magnitude in the same filter, $m_{\lambda_i} = UBVRJHK$, and

$$\sigma_i^2 = \sigma_{\text{obs},i}^2 + \sigma_{\text{mod},i}^2, \quad (3)$$

where $\sigma_{\text{obs},i}$ is the observational uncertainty. Since the RBC does not include any magnitude uncertainties, we applied the rough estimates from Galleti et al. (2004), i.e., 0.05 and 0.08 mag uncertainties for the $BVRJ$ and U bands, respectively. As for the NIR JHK magnitudes, the uncertainties are estimated as in Fan et al. (2006) by applying the relations in Fig. 2 of Carpenter, Hillenbrand & Skrutskie (2001), which shows the observed uncertainties as a function of magnitude for bright stars in the 2MASS JHK bands. In addition, Fan et al. (2006) showed that the adopted uncertainty does not affect the quality of the SED fits. $\sigma_{\text{mod},i}$ represents the uncertainty associated with the model itself, for the i^{th} filter. Following de Grijs et al. (2005) (their Sect. 3.2.4), Wu et al. (2005), Fan et al. (2006, 2010), Ma et al. (2007, 2009) and Wang et al. (2010), we adopt $\sigma_{\text{mod},i} = 0.05$.

For the 135 of 445 sample clusters without extinction values from the literature, we constrained the ages, metallicities and extinction values while keeping $[\text{Fe}/\text{H}]$ as a free parameter, using

$$\chi_{\text{min}}^2[t, [\text{Fe}/\text{H}], E(B-V)] = \min \left[\sum_{i=1}^8 \left(\frac{m_{\lambda_i}^{\text{obs}} - m_{\lambda_i}^{\text{mod}}}{\sigma_i} \right)^2 \right]. \quad (4)$$

We varied the reddening between $E(B-V) = 0.0$ and 2.0 mag in steps of 0.02 mag. We then obtained the values for the extinction coefficient, R_{λ} , by interpolating the interstellar extinction curve of Cardelli et al. (1989). We thus fitted the extinction-corrected SEDs, for which the model with the minimum χ^2 returned the best-fitting $E(B-V)$ values.

We used the same fitting method as in Fan et al. (2010). If the initial age estimate of a given star cluster is older than the *Wilkinson Microwave Anisotropy Probe* (WMAP) age of the Universe, 13.7 ± 0.2 Gyr (Spergel et al. 2003), we adopt an age of 12 Gyr as initial guess and iterate until the fitting routine reaches a local minimum. Although the estimated age could be older than 12 Gyr, this approach ensures that the estimated age will not exceed the WMAP age: see Fan et al. (2010) for details. It is well-known that SSP SEDs are not sensitive to changes in age for ages > 10 Gyr (see e.g., Ma et al. 2007, and Fig. 1). Therefore, although the upper age limit in the BS-SSP and GALEV models is 20 and 16 Gyr, respectively, the ages of the clusters determined here do not exceed the WMAP age (but see below for a discussion of the ef-

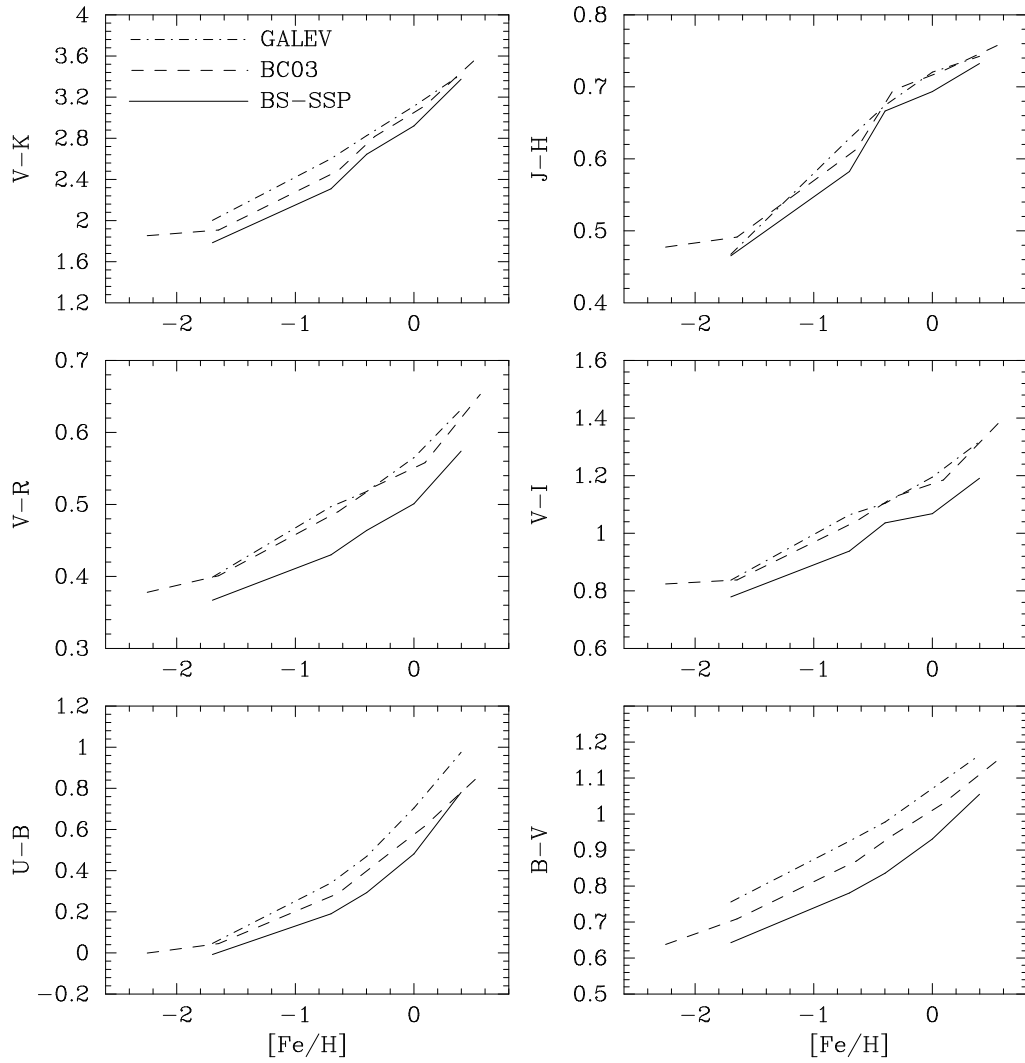


Figure 2. As Fig. 1, but for the predicted colours as a function of metallicity for 12 Gyr-old SSP models.

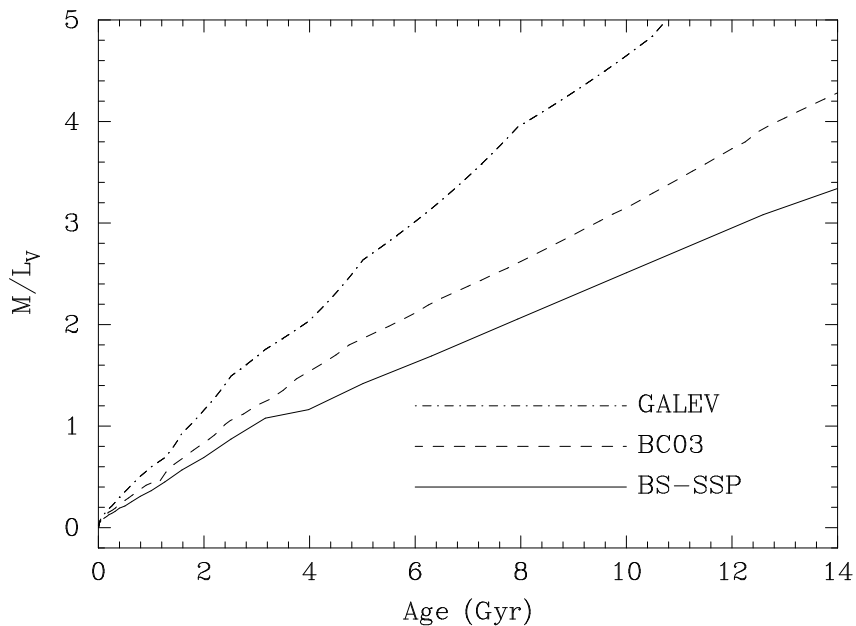


Figure 3. As Fig. 1, but for the predicted mass-to-light ratios in the V band as a function of age for solar metallicity.

fects of adopting an upper age limit in our fits). To estimate the 1σ uncertainty of a given parameter, we first fix all other parameters to their best-fitting minimum χ^2 values. We then determine $\Delta\chi^2 = \chi^2 - \chi_{\min}^2 < 1$. The confidence interval of this parameter is then given by the 1σ width of the normal distribution of $\Delta\chi^2$, which thus yields the 1σ uncertainty. We determine a cluster's mass based on the model's M/L for its specific age, metallicity and de-reddened luminosity. This is similar to the approach adopted and advocated by, e.g., Anders et al. (2004b). Since 310 of 445 clusters in our sample have robustly determined reddening values available from literature sources, only 135 of the 445 clusters may suffer more significantly from degeneracies related to the uncertain amount of extinction affecting the clusters. However, we reiterate that our NIR photometry is expected to enable us to partially break the age–metallicity degeneracy (but see Sect. 4.1). Therefore the age–metallicity–extinction degeneracy will most likely not be serious when we set the maximum model age to the WMAP age. In fact, for the BS-SSP models, 120 of our 445 clusters are older than the WMAP age, while for the BC03 and GALEV models the equivalent numbers are 55 and 99, respectively.

4 FIT RESULTS AND COMPARISONS

The fitting procedure outlined above allows us to obtain the basic parameters of our sample clusters, i.e., their ages, metallicities, masses and reddening values. Therefore, we can now compare the fit results derived based on adoption of different models and different IMFs.

4.1 Comparisons

To investigate the differences caused by adopting free versus fixed reddening, we collected data for 310 clusters with reddening values from Fan et al. (2008) and Barmby et al. (2000), and performed free- and fixed-reddening fits. We also wanted to check whether the free-reddening method could lead to degeneracies in our simultaneous age, metallicity and mass determinations.

Figure 4 shows comparisons of the extinction values, ages, metallicities and masses based on adoption of the BS-SSP models with reddening values from the literature, and those resulting from leaving reddening as a free parameter. Approximately half of the newly derived reddening values are systematically larger than the corresponding literature values. Similarly, half of the redetermined ages are in good mutual agreement for $\log(\text{age Gyr}^{-1}) > 0.4$, which indicates that the method based on leaving reddening as a free parameter may lead to a partial degeneracy in the resulting ages, since addition of NIR photometry could not break the degeneracy completely. As for the equivalent metallicity comparison, most of our results agree with one another, irrespective of the fitting method used, except that some metallicities derived from the free-reddening method are much lower than those derived based on adoption of metallicities determined previously in the literature. These results may indeed suffer from the age–metallicity–extinction degeneracy. On the other hand, the masses derived from both methods are in excellent mutual agreement in almost all cases. We also calculated the offsets and 1σ errors of the parameters derived from the free- and fixed-reddening fits: $\langle E(B - V)_{\text{free}} - E(B - V)_{\text{fixed}} \rangle = 0.115 \pm 0.233$ mag, $\langle \log \text{Age}_{\text{free}} - \log \text{Age}_{\text{fixed}} \rangle = -0.261 \pm 0.628$ [yr], $\langle [\text{Fe}/\text{H}]_{\text{free}} - [\text{Fe}/\text{H}]_{\text{fixed}} \rangle = -0.133 \pm 0.489$ dex and $\langle \log(M_{\text{free}}/M_{\odot}) - \log(M_{\text{fixed}}/M_{\odot}) \rangle = -0.039 \pm 0.202$. The systematic differences

between the free- and fixed-reddening fits is consistent with zero for all parameters.

Figure 5 shows a similar comparison as Fig. 4, but for the GALEV SSP models. In this case, the reddening values derived from the free fits, as well as the age estimates, agree better with the literature values than in Fig. 4, while the quality and mutual agreement of the mass fits is similar as in Fig. 4. However, the metallicity values derived from the free-reddening method are systematically higher than those based on fits assuming reddening values taken from the literature. We thus conclude that the age–metallicity–extinction degeneracy affecting the GALEV models is weaker than that for the BS-SSP models, but the age–metallicity–extinction degeneracy seems worse in this case than that shown in Fig. 4. Again, we calculated the offsets and 1σ uncertainties for the parameters derived from the free- and fixed-reddening fits: $\langle E(B - V)_{\text{free}} - E(B - V)_{\text{fixed}} \rangle = 0.028 \pm 0.249$ mag, $\langle \log \text{Age}_{\text{free}} - \log \text{Age}_{\text{fixed}} \rangle = -0.088 \pm 0.740$ [yr], $\langle [\text{Fe}/\text{H}]_{\text{free}} - [\text{Fe}/\text{H}]_{\text{fixed}} \rangle = 0.122 \pm 0.497$ dex, and $\langle \log(M_{\text{free}}/M_{\odot}) - \log(M_{\text{fixed}}/M_{\odot}) \rangle = 0.032 \pm 0.263$. Similar to Fig. 4, also note that the systematic differences between the free- and fixed-reddening fits are consistent with zero for all parameters.

Using Figs 4 and 5, we investigated the extent of the age–metallicity degeneracy for the free-reddening results. As in Fan et al. (2010), we conclude that there are no significant offsets between the fixed- and free-reddening results for any of the basic cluster parameters. Therefore, the free-reddening results for the 310 star clusters with reddening values from the literature will no longer be used in the remainder of this paper.

Figure 6 shows comparisons of the ages, metallicities, reddening values and masses derived from the BS-SSP and BC03 models. The filled data points with error bars in the bottom panels represent the mean values for each bin. Each case yields different results owing to the different input SSP models and different IMFs used. Note that the ages based on the BS-SSP model fits are systematically older (by ~ 0.3 dex) than those derived from the BC03 models. The results from the BS-SSP models yield higher metallicity, larger reddening and more massive clusters than those derived from the BC03 models. Since the BS-SSP models implicitly assume that BSs will affect the integrated colours, the clusters appear to be younger and more metal poor. Thus, the colours predicted by the BS-SSP models are systematically bluer than those resulting from the BC03 model suite for the same age and metallicity. Therefore, it is easy to understand that the reddening values derived from the BS-SSP models are systematically larger than those derived from BC03. In addition, the BS-SSP models lead to older ages and higher metallicities. Based on Fig. 6, we note that most of the outliers are found above the locus of equality, which may be caused by relatively large numbers of BSs in those clusters. The small number of outliers below the line of equality may be partially caused by degeneracies in the fits. Table 1 presents the systematic differences in the ages, metallicities and masses derived from the BS-SSP, GALEV and BC03 SSP models. The errors listed in the table are the errors associated with the offsets. They are defined as σ/\sqrt{N} , where σ is the standard deviation and N the number of data points. Note that the reddening fits between the BS-SSP and BC03 models are consistent with one another, i.e., we do not find any systematic differences between the reddening values derived from adoption of these models.

Figure 7 is similar to Fig. 6, but uses both the BS-SSP models and the GALEV SSP models. The ages resulting from the BS-SSP models are systematically older for $\log(\text{age yr}^{-1}) > 9.5$ ($t > 3.16$ Gyr) – see Table 1 – while for younger objects the scatter is

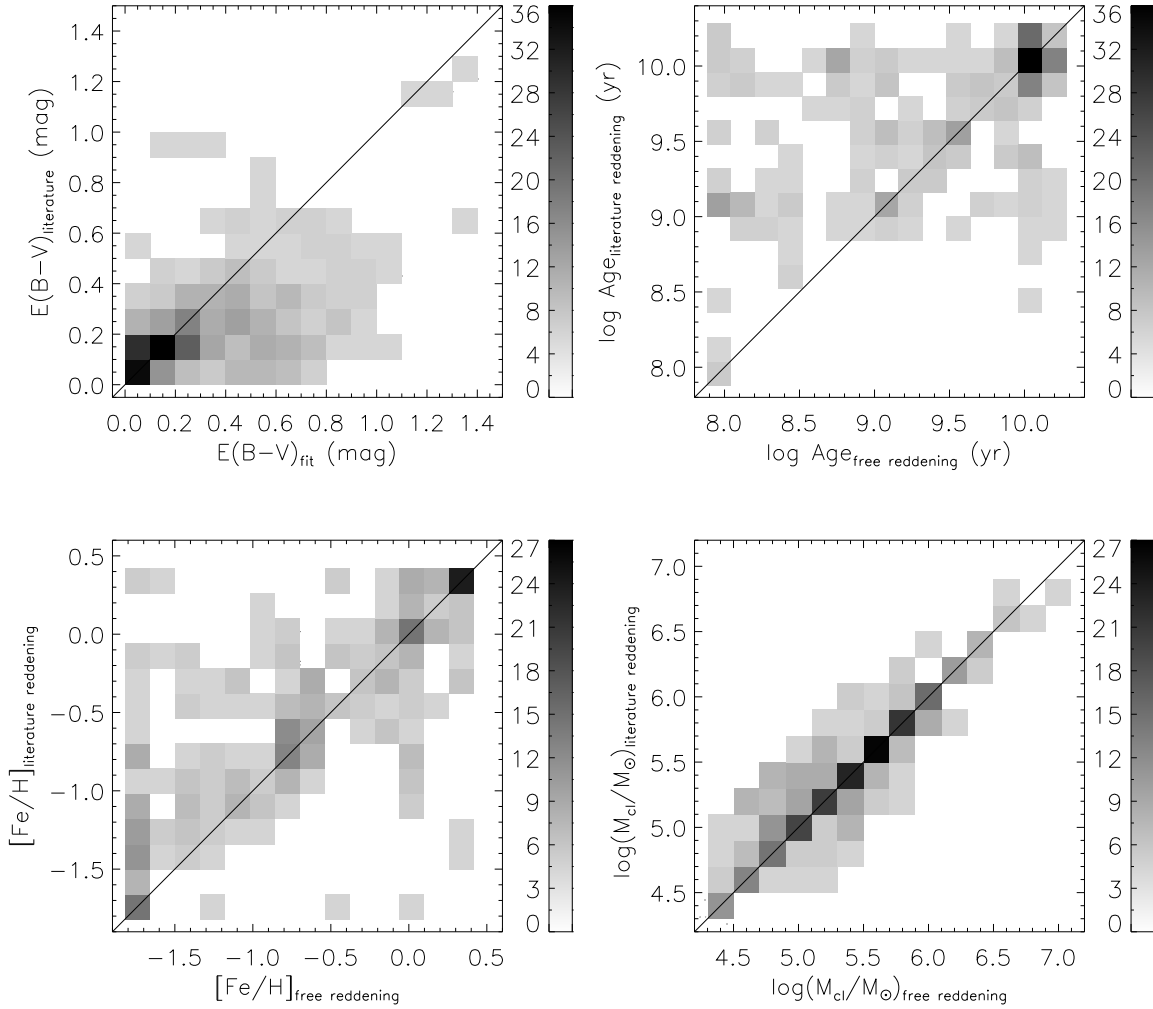


Figure 4. Comparisons of the reddening values, ages, metallicities and masses derived by adopting reddening values from the literature versus leaving extinction as a free parameter for the BS-SSP models.

Table 1. Mean offsets of the results derived from different pairs of BS-SSP, GALEV and BC03 SSP models for M31 globular-like clusters. The errors quoted are the errors associated with the offsets, defined as σ/\sqrt{N} , where σ is the standard deviation and N the number of data points.

Model suites	$\langle \Delta \log(\text{Age}) \rangle$ [yr]	$\langle \Delta [\text{Fe}/\text{H}] \rangle$ (dex)	$\langle \Delta E(B - V) \rangle$ (mag)	$\langle \Delta \log(M_{\text{cl}}) \rangle$ [M_{\odot}]
BS-SSP – BC03	0.307 ± 0.024	0.050 ± 0.024	-0.009 ± 0.006	0.200 ± 0.030
BS-SSP – GALEV	0.137 ± 0.022	0.353 ± 0.019	0.025 ± 0.006	0.091 ± 0.011
BC03 – GALEV	-0.170 ± 0.027	0.303 ± 0.025	0.035 ± 0.008	-0.109 ± 0.028

relatively large and no obvious systematic differences are seen. In addition, the metallicities resulting from the BS-SSP models are ~ 0.3 dex higher (more metal-rich) than those derived from the GALEV models. This is because the BS-SSP models correct for the effects of BSs and predict older ages and higher metallicities than the ‘standard’, single-star models. For the same reason, the resulting reddening values are higher than for the other models (since the BS-SSP models predict bluer colours). For the mass estimates, the models basically agree with one another. The presence (or absence) of BSs will thus significantly affect the fit results.

Figure 8 is the same as Fig. 6, but the comparisons of the ages, metallicities, reddening values and masses are between those derived from the BC03 models and the GALEV SSP models. The ages derived from the BC03 models are slightly younger (by 0.137 dex on average) than those derived from the GALEV models, while the metallicities derived from the BC03 model suite are significantly higher (by ~ 0.4 dex) than those based on the GALEV set for the entire metallicity range. For the masses and reddening values, the results are consistent with one another.

To check whether the differences between the results from

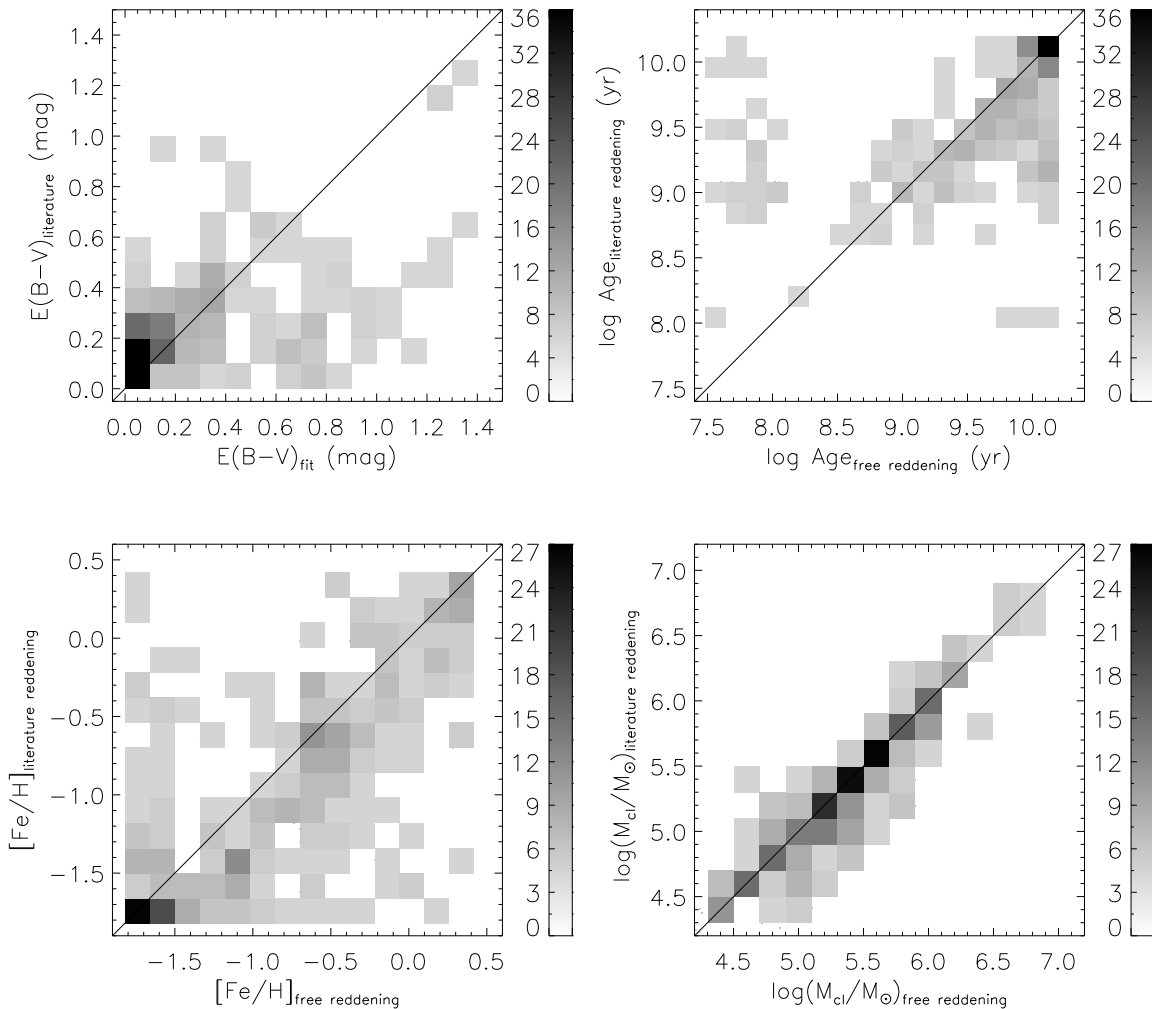


Figure 5. As Fig. 4, but for the GALEV SSP models.

the various models are caused by intrinsic differences among the models or owing to poorly understood degeneracies, we fitted the metallicities using the BS-SSP and GALEV models, adopting the same ages and reddening values as derived from the BC03 models. If the metallicities derived from the three models are the same, the differences between the results are likely caused by degeneracies in the fits; if not, differences among the models may account for the differences in the results. Figure 9 shows comparisons between the metallicities derived from the different models but adopting the ages and reddening values taken from BC03 models. Note that the metallicities are indeed different for the different models although the same ages and reddening values have been adopted. This thus shows that the differences among the results are likely caused by differences among the models. Note that this does not necessarily imply that the model differences are not caused by the age–metallicity–extinction degeneracy. We calculated the offsets between the metallicities derived from the BC03 and BS-SSP models for the ages and reddening values adopted based on application of the BC03 models: $\langle [\text{Fe}/\text{H}]_{\text{BC03}} - [\text{Fe}/\text{H}]_{\text{BS}} \rangle = -0.022 \pm 0.269$ dex. For the offsets between the metallicities from the BC03 and GALEV models with the same ages and reddening values as for

BC03 we find $\langle [\text{Fe}/\text{H}]_{\text{BC03}} - [\text{Fe}/\text{H}]_{\text{Gallev}} \rangle = 0.263 \pm 0.337$ dex. Clearly, neither offset is statistically significant.

Many recent studies show that there are systematic differences in the colours predicted by different stellar population synthesis models. Conroy & Gunn (2010) note that the Maraston (2005) models predict much redder $(J - K)$, $(V - K)$ and $(g - r)$ colours for $t < 2$ Gyr than the Bruzual & Charlot (2003) models, and that their own models are more similar to the Maraston (2005) models since the thermally pulsing asymptotic giant branch sections of the isochrone sets are comparable. Conroy & Gunn (2010) obtained old ages for the M31 and Galactic massive star clusters based on their own models, as well as on the Bruzual & Charlot (2003) and Maraston (2005) models. They found that their FSPS models can fit the NIR photometry of star clusters in the Magellanic Clouds better than the latest Padova and M05 models. The BC03 models also fit these observations quite well, although they predict NIR colours that are too blue. Conroy & Gunn (2010) also concluded that all colours – except $(J - K)$ – agree, although we note that the scatter in our M31 star cluster results is fairly large. Recently, Maraston & Stromback (2011) found that the MILES-based models predict lower fluxes in the NIR regime compared to the STELIB, Pickles or MARCS-based models. In

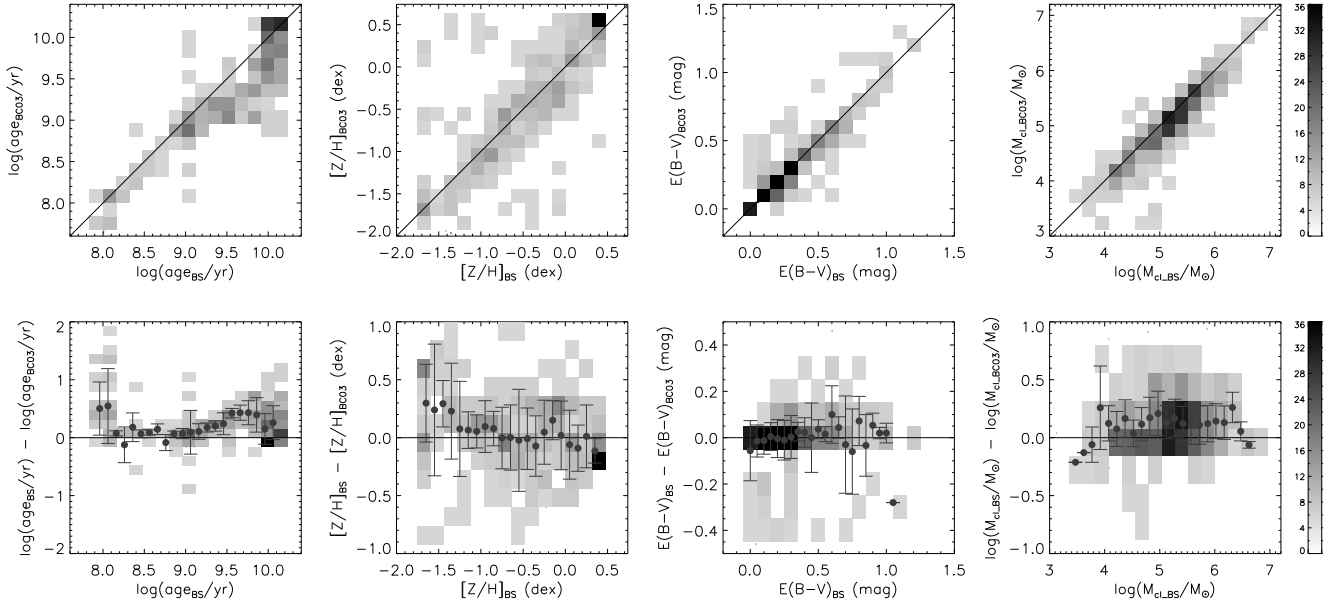


Figure 6. Comparisons of ages, metallicities, reddening values and masses derived from the BS-SSP and BC03 models. In the bottom panels, the filled data points with 1σ error bars represent the mean values of the binned data.

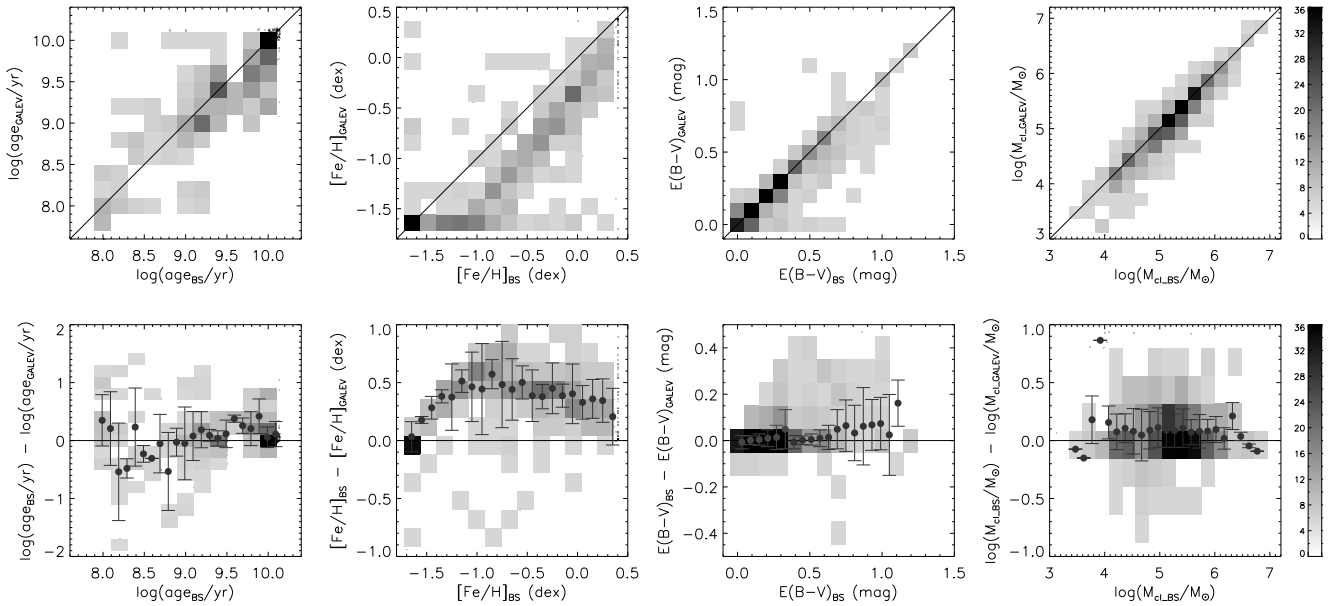


Figure 7. As Fig. 6, but for the BS-SSP and GALEV SSP models.

addition, the MILES-based models of Vazdekis et al. (2010) and Conroy & Gunn (2010) agree well with Maraston (2009). These authors found good agreement of bluer predicted colours, both in luminous red galaxies and globular clusters. They also note the good agreement between their results from full spectral fitting and colour–magnitude diagram analysis. Peacock et al. (2011) found that the Bruzual & Charlot (2003), Maraston (2005) and Padova models can fit the M31 clusters well, except the $(g - r)$ colours. Maraston & Stromback (2011)’s MILES models as well as the Vazdekis et al. (2010) models can fit the $(g - r)$ colours of the M31 star clusters very well for all metallicities.

4.2 Age, metallicity and mass distributions

The cluster age distribution is interesting, because it offers a clue to the galaxy’s formation history. Figure 10 shows the age distribution of our sample of globular-like clusters in M31 (bin size: 0.1 dex). In the top panels, the ages have been derived assuming the WMAP age of 13.7 ± 0.2 Gyr as upper limit, while in the bottom panels the ages have been fitted using the original models without imposing an upper age limit, for comparison. Clearly, for the same model, the distributions in the top and bottom panels are essentially the same for ages < 10 Gyr. However, it seems that there are more

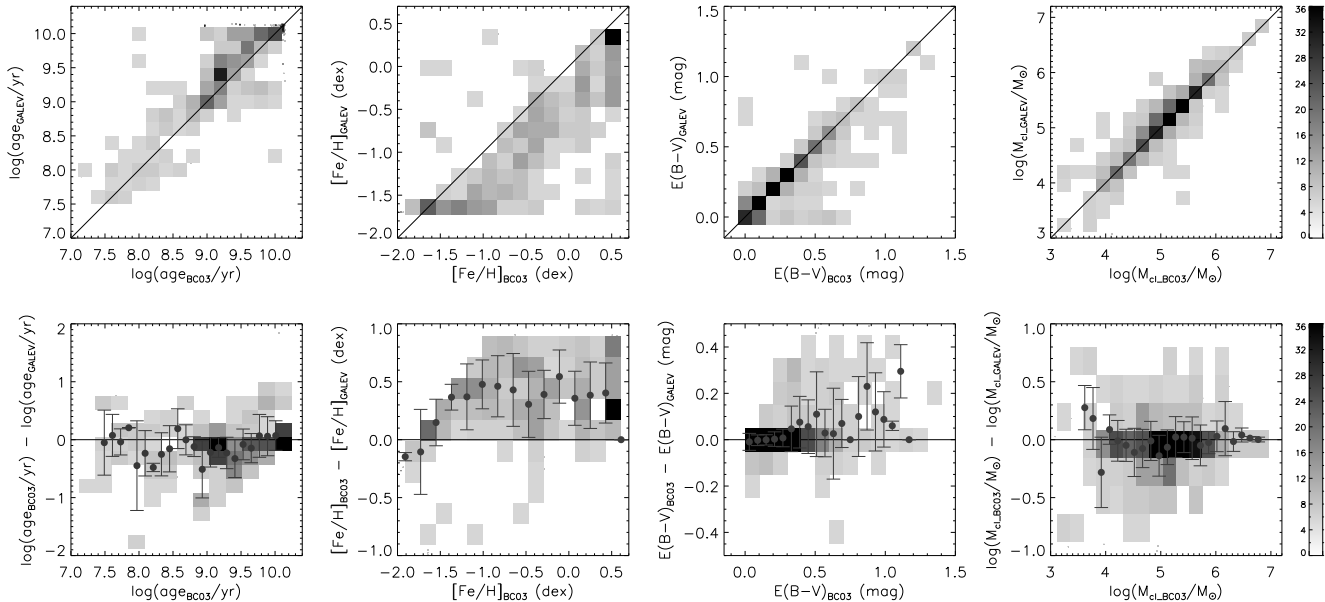


Figure 8. As Fig. 6, but for the BC03 and GALEV models.

star clusters older than the *WMAP* age in the bottom panels, which may be caused by either reddening values that have been underestimated (i.e., the age–extinction degeneracy) or observational errors. It appears that there is a larger fraction of old globular-like clusters in the distribution resulting from application of the BS-SSP models than in those of the other models, which again confirms that the BS-SSP models tend to predict older ages. If we consider the clusters older than 2 Gyr as the ‘old sample’, the relative fractions of old clusters are 67, 50 and 59 % for the BS-SSP, BC03 and GALEV models, respectively. The mean values of the histograms are given in Table 2. Note that if we adopt the BC03 models, a large fraction of clusters are aged between 1 and 10 Gyr (please see Fig. 10). The oldest age estimates are derived from the BS-SSP models, while we note that changing the IMF (Kroupa vs. Chabrier) does not evidently affect the results. There is a large fraction ($\sim \frac{1}{3}$) of young star clusters (< 2 Gyr) in our distributions. This is similar to the result of Wang et al. (2010).

The newly derived age distribution of our sample clusters, combined with that of the younger clusters reported in previous studies (e.g., Caldwell et al. 2009; Wang et al. 2010; Fan et al. 2010; Peacock et al. 2010), shows evidence of active star formation in M31 during the past 2 Gyr. This implies that there may have been several star-forming episodes in this period, possibly triggered by a major or several minor mergers with other, smaller galaxies. The age distribution of the M31 globular-like clusters is quite different from that of the Milky Way’s GCs, most of which are older than 10 Gyr (e.g., VandenBerg et al. 1996; De Angeli et al. 2005). In fact, this might be owing to our sample selection. Our results are based on observations in the M31 disc, where most of the young clusters are located. Hammer et al. (2007) suggested that the Milky Way has had an exceptionally quiet formation history during the last 10 Gyr and M31 might have undergone a recent, active merger, which may account for the observation that all Galactic GCs are old, whereas we find a large fraction of YMCs in M31. McConnachie et al. (2009) suggested that an encounter between M33 and M31 took place a few Gyr ago. The clusters with ages

Table 2. Mean values of the best-fitting age, metallicity and mass distributions based on different models.

Parameter	BS-SSP	BC03	GALEV
$\log(\text{age yr}^{-1})$	9.50	9.19	9.36
$[\text{Fe}/\text{H}]$ (dex)	-0.475	-0.525	-0.828
$\log(M_{\text{cl}}/M_{\odot})$	5.16	4.95	5.07

in excess of 10 Gyr in Fig. 10 were most likely created during the epoch when the galaxy formed, while the young globular-like clusters might have been created in a number of mergers during the last few Gyr or by the postulated recent galactic encounter with M33.

Figure 11 shows the resulting metallicity distributions based on the different SSP models for a bin size of 0.1 dex. Although the upper and lower limits of the metallicity distributions vary for the different models, the distributions are different overall and they do not exhibit any significant peaks. Table 2 lists the mean values of the metallicity distributions. We find that the choice of IMF does not significantly affect the results; the average value resulting from adoption of the GALEV models represents the lowest metallicity while that of the BS-SSP models yields the highest metallicity. The GALEV models result in a much higher fraction of metal-poor ($[\text{Fe}/\text{H}] < -1.5$) populations compared to both the BS-SSP and BC03 models. Since the lower limit in metallicity is much lower in the BC03 model suite, the corresponding distribution extends to lower metallicities.

A significant body of recent work focuses on the mass distribution of the M31 star clusters (for recent publications see, e.g., Fan et al. 2010; Wang et al. 2010). The M/L values can be obtained from the models as a function of age and metallicity. We calculated the M/L_V values using both the BS-SSP and GALEV SSP models, luminosities based on conversion of the V -band fluxes, and an M31 distance modulus of $(m - M)_0 = 24.47$ mag (McConnachie et al. 2005). Figure 12 shows the mass distributions

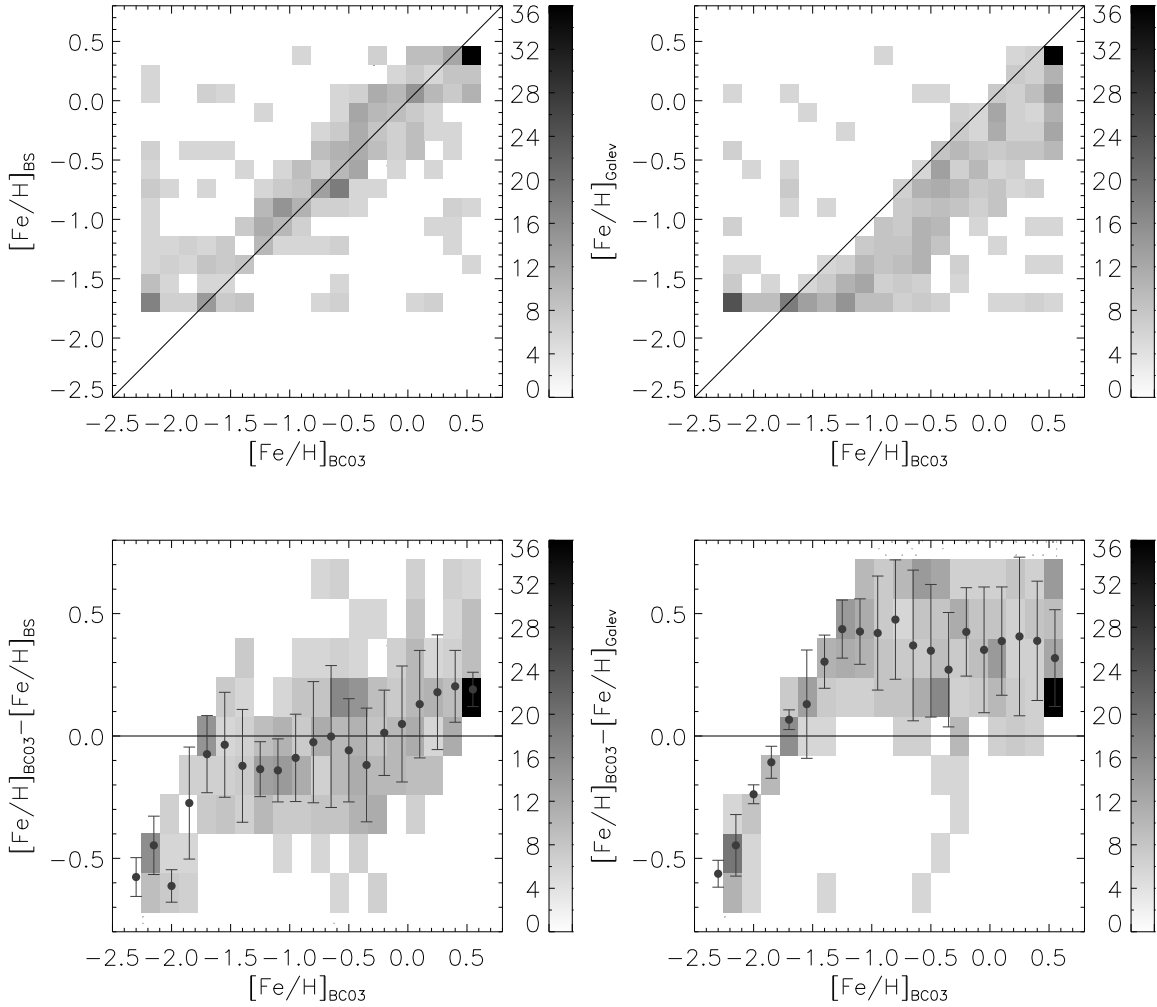


Figure 9. Comparisons between the metallicities derived from the different models but for the same ages and reddening values as derived based on the BC03 models.

of the M31 star clusters in our sample derived using the BS-SSP, GALEV and BC03 models (bin size: 0.2 dex). For each model, the mass ranges from ~ 3.4 to ~ 7 dex in units of $\log(M_{\odot})$. In addition, for comparison we also plot the mass distributions of the Galactic GCs based on the data of Harris (1996) (2010 edition; see <http://www.physics.mcmaster.ca/~harris/mwgc.dat>), assuming an age of 13 Gyr (but we remind the reader that M/L values are insensitive to age differences for such old ages). The models applied are the same as those used for the M31 star clusters. We find that the mass distributions of the M31 star clusters and the Galactic GCs are very similar, irrespective of IMF choice. Note that all mass distributions have similar peak values, from $\log(M_{cl}/M_{\odot}) = 5.0$ to 5.5, which agrees very well with the universal GC mass function, i.e., a Gaussian function with a mean of $\log(M_{cl}/M_{\odot}) \simeq 5.2$ –5.3 and a 1σ standard deviation of $\sigma_{\log(M_{cl}/M_{\odot})} \simeq 0.5$ –0.6, as suggested by Parmentier & Gilmore (2007). Table 2 lists the mean values of the distributions in Fig. 12. We find that the BS-SSP models result in the most massive mean value, while the BC03 models yield the lowest mean mass.

5 SUMMARY AND CONCLUSIONS

In this paper, we aimed at exploring the cause(s) of systematic differences among model results based on application of different SSP model suites, we have rederived the ages, metallicities, reddening values and masses of 445 M31 star clusters using χ^2 minimisation and adoption of the BS-SSP and GALEV SSP models. Our cluster sample as well as the optical broad-band and NIR photometry used were taken from Fan et al. (2010). We also compared the SED-matching results for the same sample based on the ‘standard’ single-star BC03 SSP models.

We compared the $UBVRIJHK$ colours as a function of age predicted by different SSP models, specifically the BS-SSP models with a Chabrier-like IMF, the BC03 models with a Chabrier IMF, and the GALEV models with a Kroupa IMF. We found that the BS-corrected models exhibit offsets towards bluer colours for all colours, although these offsets tend to become negligible for ages < 2 Gyr. However, note that the GALEV models show much redder colours in $(V - K)$ and $(J - H)$ for ages < 2 Gyr, which may affect age estimates for young stellar populations. The GALEV and BC03 models predict similar colours in $(U - B)$, $(B - V)$, $(V - R)$ and $(V - I)$, while both models exhibit significant offsets

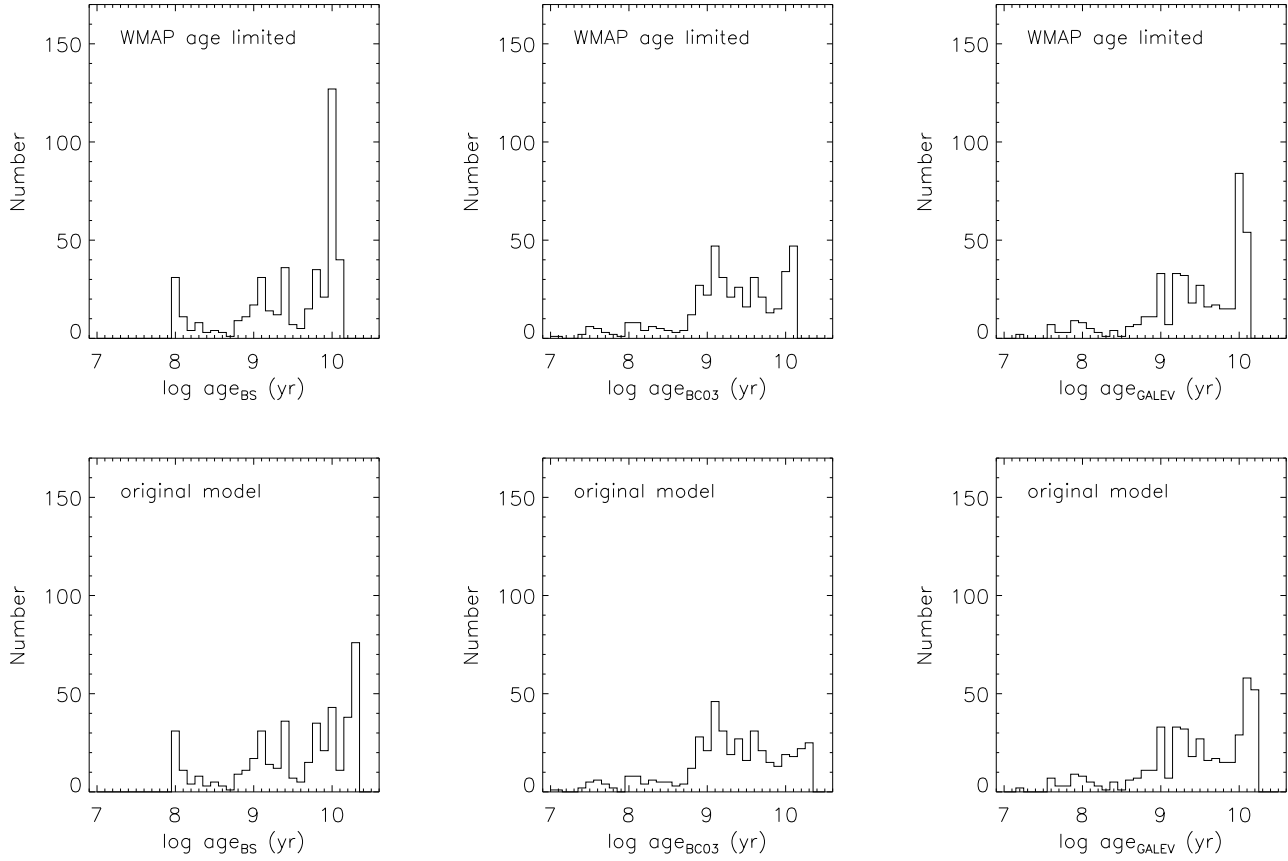


Figure 10. Age distributions for different models with different IMFs. *Top:* Ages derived from the models assuming the *WMAP* upper age limit. *Bottom:* Ages derived from the original models without imposing an upper age limit.

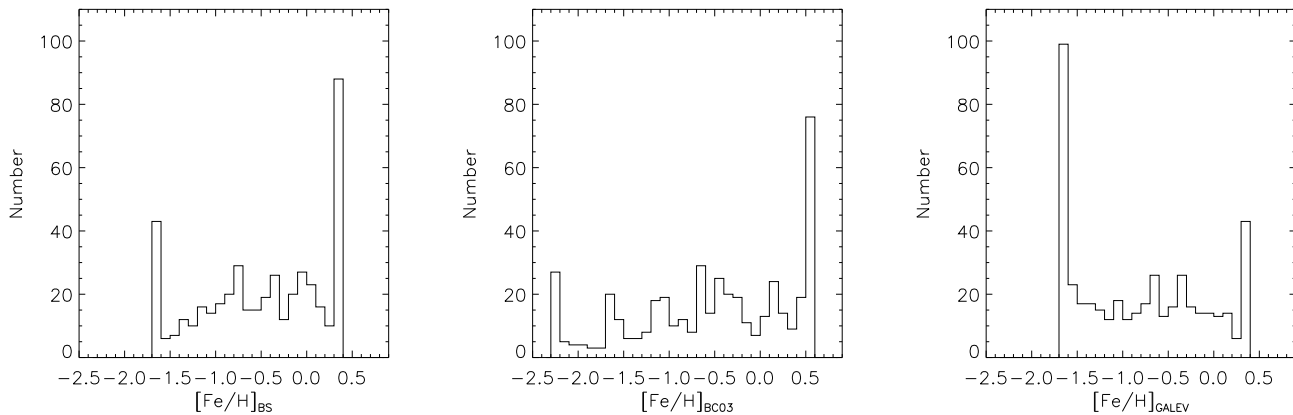


Figure 11. Metallicity distributions for different models.

in $(V - K)$ and $(J - H)$, especially for young ages. The BS-SSP models predict the bluest colours while the GALEV models predict the reddest colours. We also found that the GALEV models predict the highest M/L_s , while the BS-SSP models predict the lowest values. In addition, the differences become larger for older ages.

Our comparisons show that a reasonable choice of IMF does not affect the results significantly and that the main differences

in the results are caused by intrinsic differences among the SSP models. The ages derived from the BC03 models are the youngest while those resulting from the BS-SSP models are the oldest. For the metallicity, the results of GALEV models are the lowest while those from the BS-SSP models are the highest. Finally, the masses based on the BC03 models are the lowest and those from the BS-SSP models are the highest.

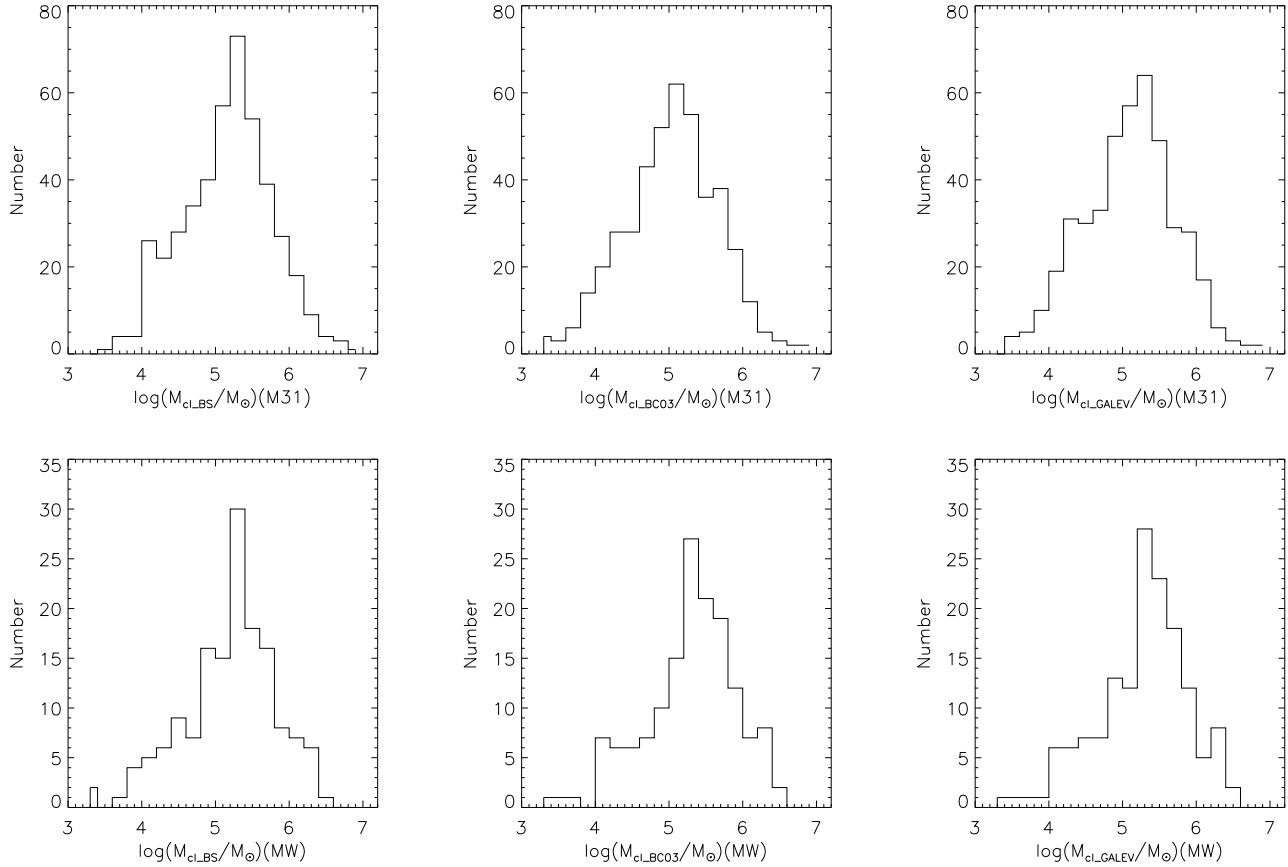


Figure 12. Cluster mass distributions for different models. *Top:* M31 star clusters. *Bottom:* Galactic star clusters.

We used photometry in eight filters (*UBVR1JHK*) for most of our sample clusters, where the *U* band and the NIR *JHK* filters are essential to obtain robust results by means of SED fits (see Sect. 3.1). We also make a case for proper inclusion of the effects of BSs in SSP codes.

ACKNOWLEDGMENTS

We are indebted to the referee for his/her thoughtful comments and insightful suggestions that improved this paper greatly. This research was supported by the National Natural Science Foundation of China (NSFC) under grants No. 11003021, 11043006, 11073001 and 11073032.

REFERENCES

- Ahumada, J., Lapasset, E., 1995, *A&As*, 109, 375
 Anders P., Fritze-v. Alvensleben U., 2003, *A&A*, 401, 1063
 Anders, P., Fritze-v. Alvensleben, U., de Grijs, R., 2003a, *ASPC*, 296, 567
 Anders, P., Fritze-v. Alvensleben, U., 2003b, *A&A*, 401, 1063
 Anders P., de Grijs R., Fritze-v. Alvensleben U., & Bissantz N., 2004a, *MNRAS*, 347, 17
 Anders, P., Bissantz, N., Fritze-v. Alvensleben, U. & de Grijs R., 2004b, *MNRAS*, 347, 196
 Arimoto, N., 1996, *From Stars to Galaxies*, Leitherer C., Fritze-v. Alvensleben U., Huchra J., eds., *ASP Conf. Ser.*, (ASP: San Francisco), 98, p287
 Ascenso, J., Alves, J., Beletsky, Y., & Lago, M. T. V. T. 2007a, *A&A*, 466, 137
 Ascenso, J., Alves, J., Vicente, S., & Lago, M. T. V. T. 2007b, *A&A*, 476, 199
 Barmby, P., et al. 2000, *AJ*, 119, 727
 Barmby, P., & Huchra, J. P. 2001, *AJ*, 122, 2458
 Barmby, P., et al. 2009, *AJ*, 138, 1667
 Bastian, N., Gieles, M., Lamers, H. J. G. L. M., Scheepmaker, R. A., de Grijs, R. 2005a, *A&A*, 431, 905
 Bastian, N., Gieles, M., Efremov, Yu. N., Lamers, H. J. G. L. M. 2005b, *A&A*, 443, 79
 Battistini, P., Bónoli, F., Braccisi, A., Fusi-Pecchi, F., Malagnini, M. L., & Marano, B. 1980, *A&As*, 42, 357
 Battistini, P., Bónoli, F., Braccisi, A., Federici, L., Fusi Pecci, F., Marano, B., & Borngen, F. 1987, *A&As*, 67, 447
 Battistini, P., Bónoli, F., Casavecchia, M., Ciotti, L., Federici, L., & Fusi Pecci, F. 1993, *A&A*, 272, 77
 Bruzual, G., & Charlot, S. 1993, *ApJ*, 405, 538
 Bruzual, G., & Charlot, S. 2003, *MNRAS*, 344, 1000 (BC03)
 Caldwell, N., Harding, P., Morrison, H., Rose, J. A., Schiavon, R., & Kriessler, J. 2009, *AJ*, 137, 94
 Cardelli, J. A., Clayton, G. C., & Mathis, J. S. 1989, *ApJ*, 345, 245
 Carpenter, J. M., Hillenbrand, L. A., & Skrutskie, M. F. 2001, *AJ*,

- 121, 3160
- Cenarro, A. J., Cervantes, J. L., Beasley, M. A., Marin-Franch, A., & Vazdekis, A., 2008, *ApJ*, 689, L29
- Chabrier, G. 2003, *PASP*, 115, 763
- Charlot, S., & Bruzual, G. 1991, *ApJ*, 367, 126
- Conroy, C., Gunn, J. E., White, M. 2009, *ApJ*, 699, 486
- Conroy, C., & Gunn, J. E. 2010, *ApJ*, 712, 833
- Crampton, D., Cowley, A. P., Schade, D., & Chayer, P. 1985, *ApJ*, 288, 494
- De Angeli, F., et al. 2005, *AJ*, 130, 116
- de Grijs, R., Bastian, N., & Lamers, H. J. G. L. M. 2003, *MNRAS*, 340, 197
- de Grijs, R., Fritze-v. Alvensleben, U., Anders, P., Gallagher, J. S., Bastian, N., Taylor, V. A., Windhorst, R. A. 2003, *MNRAS*, 342, 259
- de Grijs, R., et al. 2004, *MNRAS*, 352, 263
- de Grijs, R., et al. 2005, *MNRAS*, 359, 874
- de Grijs, R., & Anders, P. 2006, *MNRAS*, 366, 295
- Fan, X., et al. 1996, *AJ*, 112, 628
- Fan, Z., Ma, J., de Grijs, R., Yang, Y., & Zhou, X. 2006, *MNRAS*, 371, 1648
- Fan, Z., Ma, J., de Grijs, R., & Zhou, X. 2008, *MNRAS*, 385, 1973
- Fan, Z., de Grijs, R., & Zhou, X. 2010, *ApJ*, 725, 200
- Fioc, M., & Rocca-Volmerange, B. 1997, *A&A*, 326, 950
- Frayn, C. M., & Gilmore, G. F. 2002, *MNRAS*, 337, 445
- Fritze-v. Alvensleben, U., Bicker, J. 2006, *A&A*, 454, 67
- Galleti, S., Federici, L., Bellazzini, M., Fusi Pecci, F., & Macrina, S. 2004, *A&A*, 416, 917
- Galleti, S., Federici, L., Bellazzini, M., Buzzoni, A., & Fusi Pecci, F. 2006, *A&A*, 456, 985
- Galleti, S., Bellazzini, M., Federici, L., Buzzoni, A., & Fusi Pecci, F. 2007, *A&A*, 471, 127
- Galleti, S., Bellazzini, M., Buzzoni, A., Federici, L., Fusi Pecci, F. 2009, *A&A*, 508, 1285
- Gieles, M., Bastian, N., Lamers, H. J. G. L. M., Mout, J. N., 2005, *A&A*, 441, 949
- Hammer, F., Puech, M., Chemin, L., Flores, H., & Lehnert, M. D. 2007, *ApJ*, 662, 322
- Harris, W. E. 1996, *AJ*, 112, 1487.
- Hodge, P., Krienke, O. K., Bianchi, L., Massey, P., Olsen, K. 2010, *PASP*, 122, 745
- Hubble, E. 1932, *ApJ*, 76, 44
- Hunter, D. A., O'Connell, R. W., Gallagher, J. S., III 1994, *AJ*, 108, 84
- Jiang, L., Ma, J., Zhou, X., Chen, J., Wu, H., & Jiang, Z. 2003, *AJ*, 125, 727
- Kaviraj, S., Rey, S. C., Rich, R. M., Lee, Y. W., Yoon, S. J., Yi, S. K. 2007, *MNRAS*, 381, 74
- Kotulla, R., Fritze, U., Weilbacher, P., & Anders, P. 2009, *MNRAS*, 396, 462.
- Krienke, O. K., & Hodge, P. W. 2007, *PASP*, 119, 7
- Kroupa, P. 2001, *MNRAS*, 322, 231
- Kurucz, R. L. 1992, in *IAU Symp. 149, The Stellar Populations of Galaxies*, ed. B. Barbuy & A. Renzini (Dordrecht: Kluwer), 225
First citation in article
- Lejeune, T., Cuisinier, F., & Buser, R. 1997, *A&As*, 125, 229
- Lejeune, T., Cuisinier, F., & Buser, R. 1998, *A&As*, 130, 65
- Leitherer, C., & Heckman, T. M. 1995, *ApJS*, 96, 9
- Ma, J., et al. 2007, *ApJ*, 659, 359
- Ma, J., et al. 2009, *AJ*, 137, 4884
- Macri L. M. 2001, *ApJ*, 549, 721
- Maíz Apellániz J., 2009, *ApSS*, 324, 95
- Maraston, C. 1998, *MNRAS*, 300, 872
- Maraston, C. 2005, *MNRAS*, 362, 799
- Maraston, C., Nieves Colmenarez, L., Bender, R., Thomas, D. 2009, *A&A*, 493, 425
- Maraston, C., & Stromback, G. 2011, *MNRAS*, 418, 2785
- Massey, P., Olsen, K. A. G., Hodge, P. W., Strong, S. B., Jacoby, G. H., Schlingman, W., & Smith, R. C. 2006, *AJ*, 131, 2478
- McConnachie, A. W., et al. 2005, *MNRAS*, 356, 979
- McConnachie, A. W., et al. 2009, *Nature*, 461, 66
- McCradly, N. 2009, *Ap&SS*, 324, 109
- Moll, S. L., de Grijs, R., Mengel, S., & Smith, L. J. 2008, *ASPC*, 388, 411
- O'Connell, R. W., Mangano, J. J. 1978, *ApJ*, 221, 62
- Parmentier, G., & Gilmore, G. 2007, *MNRAS*, 377, 352
- Peacock, M. B., Maccarone, T. J., Knigge, C., Kundu, A., Waters, C. Z., Zepf, S. E., & Zurek, D. R. 2010, *MNRAS*, 402, 803
- Peacock, M. B., Zepf, S. E., Maccarone, T. J., & Kundu, A. 2011, *MNRAS*, 737, 5
- Perina, S., et al. 2010, *A&A*, 494, 933
- Perina, S., et al. 2010, *A&A*, 511, 23
- Piotto, G., et al. 2002, *A&A*, 391, 945
- Salpeter E. E. 1955, *ApJ*, 121, 161
- Sargent, W. L. W., Kowal, C. T., Hartwick, F. D. A., & van den Bergh, S. 1977, *AJ*, 82, 947
- Schulz, J., Fritze-v. Alvensleben, U., Moller, C. S., Fricke, K. J. 2002, *A&A*, 392, 1
- Schulz, J., Fritze-v. Alvensleben, U., Fricke, K. J. 2003, *A&A*, 398, 89
- Smith, L. J., Kowal, et al. 2007, *ApJ*, 667, L145
- Spergel, D. N., et al. 2003, *ApJS*, 148, 175
- Stanek, K. Z., & Garnavich, P. M. 1998, *ApJ*, 503, 131
- VandenBerg, D. A., Bolte, M., Stetson, P. B. 1996, *ARA&A*, 34, 461
- Vazdekis, A. 1999, *ApJ*, 513, 224
- Vazdekis, A., et al. 2010, *MNRAS*, 404, 1639
- Vetešník, M. 1962, *Bulletin of the Astronomical Institutes of Czechoslovakia*, 13, 180
- Wang, S., Fan, Z., Ma, J., de Grijs, R., & Zhou, X. 2010, *AJ*, 139, 1438
- Whitmore, B., et al. 2005, *AJ*, 130, 2104
- Worthey, G. 1994, *ApJs*, 95, 107
- Wu, H., Shao, Z. Y., Mo, H. J., Xia, X. Y., & Deng, Z. G. 2005, *ApJ*, 622, 244
- Xin, Y., & Deng, L., 2005, *ApJ*, 619, 824
- Xin, Y., Deng, L., & Han, Z. W., 2007, *ApJ*, 660, 319
- Xin, Y., Deng, L. C., de Grijs, R., & Kroupa, P. 2011, *MNRAS*, 411, 761
- Yi, S. K., Kim, Y. C., & Demarque, P. 2003, *ApJS*, 144, 259